Phase-tunable electron transport assisted by odd-frequency Cooper pairs in topological Josephson junctions

Jorge Cayao [ORCID],[1] Paramita Dutta [ORCID],[2] Pablo Burset [ORCID],[3] and Annica M. Black-Schaffer [ORCID][1]

[1]*Department of Physics and Astronomy, Uppsala University, Box 516, S-751 20 Uppsala, Sweden*
[2]*Theoretical Physics Division, Physical Research Laboratory, Navrangpura, Ahmedabad-380009, India*
[3]*Department of Theoretical Condensed Matter Physics, Condensed Matter Physics Center (IFIMAC) and Instituto Nicolás Cabrera,
Universidad Autónoma de Madrid, 28049 Madrid, Spain*

We consider a finite-size topological Josephson junction formed at the edge of a two-dimensional topological insulator in proximity to conventional superconductors and study the impact of Cooper pair symmetries on the electron transport. We find that, due to the finite junction size, electron transport is highly tunable by the superconducting phase difference ϕ across the junction. At zero frequency and $\phi = \pi$, the setup exhibits vanishing local Andreev reflection and perfect normal transmission due to the interplay of finite junction size and formation of topological Andreev bound states in the middle of the junction. We reveal that this striking behavior enables odd-frequency Cooper pairs to become the only type of pairing inside the topological junction that contribute to transport. Our paper thus offers a highly tunable detection scheme for odd-frequency Cooper pairs.

Engineering superconducting states with unique functionalities has lately triggered great interest, not only due to their unexpected properties but also owing to their potential for quantum technologies [1]. Odd-frequency superconductivity is an interesting but less explored superconducting state where the basic units, the Cooper pairs, are formed by two electrons at different times. These odd-frequency Cooper pairs are characterized by a wave function, or *pair amplitude*, that is *odd* in the relative time, or frequency ω, of the paired electrons [2–5]. Initially, the odd-frequency (odd-ω) state was predicted as an intrinsic effect [6–8], but later it was found that it can be engineered using simple conventional s-wave superconductors [9,10].

Heterostructures based on conventional superconductors have been shown to be the simplest and experimentally most relevant platform for odd-ω pairing [9–29]. In these systems, breaking the translational invariance at interfaces serves as a source of odd-ω pairs [5]. In the additional presence of spin mixing fields, e.g., from magnetism or spin-orbit coupling, the even- and odd-ω pairs can acquire spin-singlet and -triplet symmetries, respectively, even when using conventional superconductors [14,30–38]. In all these systems, odd-ω pairs have provided fundamental understanding of the proximity-induced superconductivity [2,3,5,39] and have also enabled the entire field of superconducting spintronics [40–43]. Despite all the advances, however, there are still sev-

eral critical questions that remain unresolved. First, in many cases, the appearance of odd-ω pairing is also accompanied by an even-ω component that easily obscures the effect of the odd-ω part, see e.g., Refs. [2,5,10]. Second, most detection protocols involve observables, such as the local density of states, that do not directly measure pair correlations [28,35]. Third, the majority of previous work, including experiments, have mainly used heterostructures with magnetic materials [24,28,39,44,45], which can easily become rather challenging as magnetism is detrimental for superconductivity.

With the advent of topological superconductors [46], the spectral bulk-boundary correspondence [47] predicted a different route for large odd-ω pairs, thus avoiding some of the previous problems. Topological superconductors have lately attracted great interest not only because they represent another state of matter but also because they host Majorana zero modes (MZMs) [46], which are promising candidates for fault-tolerant quantum computation [48]. Perhaps the most appealing way to realize topological superconductivity without magnetism combines conventional superconductors and two-dimensional topological insulators (2DTIs) [49,50]; see also Refs. [51–54]. 2DTIs have intrinsic strong spin-orbit coupling and host metallic 1D edge states which only experience Andreev reflections in normal-superconductor (NS) 2DTI-based heterostructures [55–61]. These Andreev processes have recently been shown to generate odd-ω spin-triplet pairs [14,16,21,22], notably without the presence of magnetic fields, but still accompanied by even-ω pairs that have so far challenged the identification of odd-ω pairing. As a consequence, despite large interest in odd-ω pairs, the generation of pure odd-ω pairs and their detection still represent two open critical problems.

In this paper, we consider a finite Josephson junction formed at the edge of a 2DTI and identify the Cooper pair
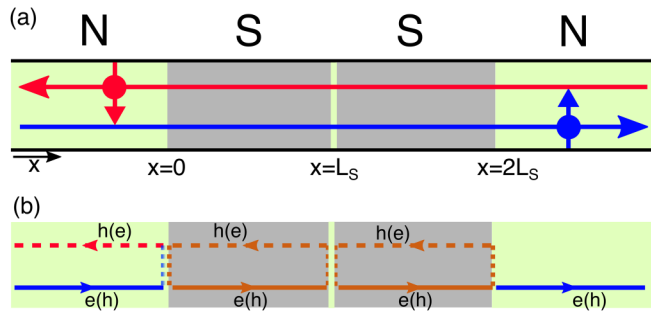
(a)

FIG. 1. (a) Sketch of N-SNS-N junction at the 1D metallic edge of a 2DTI, with N (S) regions colored green (gray) and a middle N region of vanishing length. The S regions have finite lengths (L_S) and order parameters, with Δ and $\Delta\,e^{i\phi}$ for the left and right S regions, respectively. Horizontal red and blue arrows depict the counterpropagating edge modes carrying opposite spin (vertical arrows). (b) An injected electron (hole) from the leftmost N can be Andreev reflected (dashed lines) or transmitted (solid lines) into the rightmost N as an electron due to the helical nature of the 2DTI.

symmetries responsible for the electron transport observables. In particular, we focus on N-SNS-N junctions with a very short middle N region and finite S regions, where superconductivity is proximity-induced from conventional superconductors and where an external flux controls the superconducting phase difference (ϕ) between them, see Fig. 1(a). Interestingly, we obtain vanishing local Andreev reflection and perfect normal transmission at frequency $\omega = 0$ and phase $\phi = \pi$ as a result of the interplay between the formation of a pair of topological Andreev bound states (ABSs) and the finite junction size. We reveal that this behavior is accompanied by the emergence of *only* odd-ω mixed spin-triplet pairs in the middle of the junction, thus unveiling the Cooper pair symmetry that determines transport in this special regime. Since the helicity constraints make the Andreev reflection and normal transmission directly set the local and nonlocal conductances, respectively, we conclude that electron transport provides an excellent and controllable way to detect odd-ω pairs in 2DTI Josephson junctions.

I. 2DTI JOSEPHSON JUNCTION

We consider a N-SNS-N junction at the edge of a 2DTI with N being normal-state regions and S being regions in contact with conventional spin-singlet *s*-wave superconductors, see Fig. 1(a). For simplicity, we assume a middle N region of vanishing length and S regions of the same length L_S, with the interfaces located at $x = 0, L_S, 2L_S$. This effectively 1D system is then modeled by the Bogoliubov-de Gennes (BdG) Hamiltonian,

$$H_{BdG} = v_F p_x \tau_z \sigma_z - \mu \tau_z + \mathbf{\Delta}(x)\tau_x, \qquad (1)$$

in the basis $\Psi(x) = (\psi_\uparrow, \psi_\downarrow, \psi_\uparrow^\dagger, -\psi_\uparrow^\dagger)^T$, where T denotes the transpose operation and $\psi_\sigma^\dagger(x)$ adds an electron with spin $\sigma = \uparrow, \downarrow$ at position x along the edge. The first term in Eq. (1) represents the 1D metallic edge of a 2DTI [50,62–65], where the spin quantization direction is along the z axis, $p_x = -i\hbar\partial_x$, v_F is the Fermi velocity of the edge state, and σ_i (τ_i) is the *i*th Pauli matrix in spin (Nambu) space. Without loss of

generality, we assume $\hbar = 1$, $v_F = 1$ [64]. Next, μ is the chemical potential and the last term, $\mathbf{\Delta}(x)$, is the induced superconducting order parameter at the edge of the 2DTI, which is $\mathbf{\Delta}(x) = 0$ in the N regions, $\mathbf{\Delta}(x) = \Delta$ in the left S, and $\mathbf{\Delta}(x) = \Delta e^{i\phi}$ in the right S. Here, ϕ is the superconducting phase and Δ the order parameter amplitude which introduces the superconducting coherence length $\xi = v_F/\Delta$. We note that a finite ϕ, combined with the 2DTI helicity, enables the formation of topological ABSs and the emergence of MZMs at $\phi = \pi$ [50,66]. As we will see, these topological properties are strongly affecting the behavior of the Josephson junction studied here.

We are interested in studying the induced Cooper pair symmetries and their impact on transport across the N-SNS-N junction in Fig. 1 and modeled by Eq. (1). In the following, we first determine the equilibrium transport based on scattering processes which we then employ to identify the induced Cooper pair symmetries and their impact on transport signatures. To highlight the physics, we here discuss the results and present the detailed calculations in the Supplemental Material [67].

II. TRANSPORT SIGNATURES

To begin, we identify the microscopic scattering processes responsible for reflections on one side of the Josephson junction and transmissions across it, which define the measurable local and nonlocal conductances of the junction; see Fig. 1. Due to the 2DTI helicity, normal reflections and crossed Andreev reflections are forbidden [53,68,69]: a right-moving electron (hole) from the leftmost N region [blue solid arrow in Fig. 1(b)] can only be reflected as a hole (electron) at the NS interface at $x = 0$. This process, known as local Andreev reflection, results in the creation (annihilation) of a Cooper pair in S and we characterize it by the amplitude $r_{eh(he)}$. The right-moving electron (hole) can also be transmitted, ultimately all the way to the rightmost N, but only as an electron (hole) [blue solid arrow in Fig. 1(b)]; a process known as normal transmission and here characterized by $t_{ee(hh)}$. As a consequence, only the local Andreev reflection $r_{eh(he)}$ and normal transmission $t_{ee(hh)}$ determine local and nonlocal conductances, respectively, across the junction. In particular, at zero temperature the local conductance in the leftmost N region after applying a bias voltage $V > 0$ ($V < 0$) is related to the Andreev reflection as $\sigma_{LL} = (e^2/h)(1 + |r_{eh(he)}|^2)$ per spin channel. The nonlocal conductance, measured in the rightmost N region for the same bias, is related to normal transmission as $\sigma_{LR} = (e^2/h)|t_{ee(hh)}|^2$ per spin channel. In the following, it is sufficient to study $r_{eh(he)}$ and $t_{ee(hh)}$, which we obtain by matching the scattering states of the system at all its interfaces [67].

In Figs. 2(a) and 2(c), we plot the total local Andreev reflection $|R|^2 = |r_{eh}|^2 + |r_{he}|^2$ and the total transmission $|T|^2 = |t_{ee}|^2 + |t_{hh}|^2$ as a function of frequency ω and phase difference ϕ. In Figs. 2(b) and 2(d), we additionally show $|r_{eh}|^2$ and $|t_{ee}|^2$ as a function of ω at $\phi = 0, \pi$. The first observation is that these scattering processes acquire a strong phase dependence for $|\omega| < \Delta$. In fact, R and T develop regions that strongly depend on ϕ and follow a cosine profile that reflects the formation of the pair of topological ABSs at $x = L_S$, known to emerge in 2DTI Josephson junctions
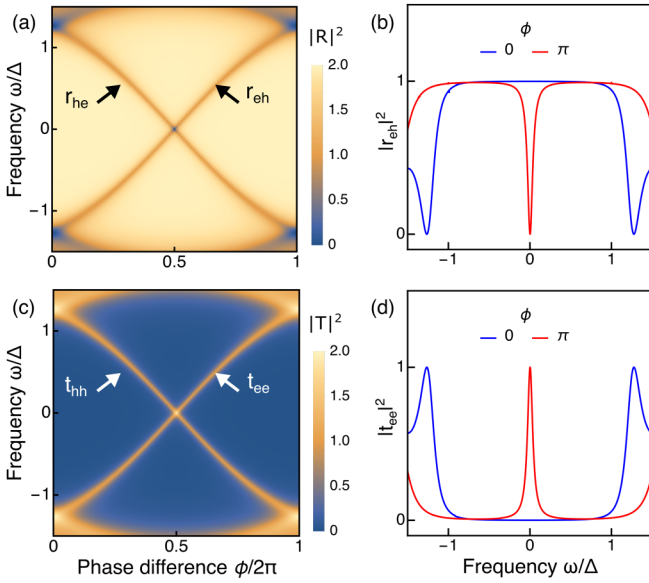
FIG. 2. Scattering probabilities. (a) Total Andreev reflection probability $|R|^2 = |r_{eh}|^2 + |r_{he}|^2$ due to the incidence of an electron (r_{eh}) and a hole (r_{he}) from the leftmost N region as a function of ω and ϕ; black arrows indicate the phase-dependent branches from $r_{eh(he)}$. (b) Andreev probability, $|r_{eh}|^2$, as a function of frequency at $\phi = 0, \pi$. (c), (d) Same as (a), (b) but for the transmission $|T|^2 = |t_{ee}|^2 + |t_{hh}|^2$ to the rightmost N region. Parameters: $\mu = \Delta, L_S = 2\xi$.

[50]. The signature of these ABSs in R and T occurs because the scattering amplitudes are heavily dependent on the poles of the scattering matrix, which gives the conditions for the formation of bound states in a scattering system, see, e.g., Refs. [21,70,71]. The key property of topological ABSs is that, due to the helicity, they develop a zero-frequency crossing at $\phi = \pi$, which is protected by the conservation of the total fermion parity and signals the emergence of MZMs. We further note that even when the middle N region of the topological Josephson junction in Fig. 1 has a finite length and hosts additional pairs of ABSs within the gap, the low-energy results presented here remain unchanged [21,72–74]. This property can be also seen by noting that each ABS emerges from a distinct Andreev process, r_{eh} and r_{he} [black arrows in Fig. 2(a)], which gives rise to a protected zero-frequency crossing at $\phi = \pi$ [the same holds for $|T|^2$ in (c)]. The fact that local Andreev reflection and normal transmission capture the topological ABSs is a remarkable property, as it implies that they can be easily detected in local and nonlocal conductances. The second observation is that the strong phase dependence of the total Andreev reflection R and transmission T reveals a very distinct behavior at $\phi = \pi$ when $\omega = 0$. This regime is here of particular interest as it is a key property of topological ABSs [50]. To further understand the very distinct behavior of R and T in this regime, we derive the analytical expressions for the Andreev and transmission amplitudes at $\omega = 0$,

$$r_{eh}(\omega = 0) = \frac{1}{2i} \frac{(1 + e^{-i\phi})\sinh(2L_S/\xi)}{\sinh^2(L_S/\xi)e^{-i\phi} + \cosh^2(L_S/\xi)},$$

$$t_{ee}(\omega = 0) = \frac{1}{\sinh^2(L_S/\xi)e^{-i\phi} + \cosh^2(L_S/\xi)}, \quad (2)$$

with $r_{he}(\phi) = r_{eh}(-\phi)$ and $t_{hh}(\phi) = t_{ee}(-\phi)$. At $\phi = 0$, the Andreev reflection is in fact constant for frequencies $|\omega| < \Delta$, becoming $r_{eh} = 1$ when $2L_S \gg \xi$, while t_{ee} instead vanishes in this regime, see blue curves in Figs. 2(b) and 2(d). In contrast, at $\phi = \pi$, the Andreev reflection and transmission develop, respectively, a dip reaching $r_{eh} = 0$ and a resonant peak $t_{ee} = 1$ at $\omega = 0$, surprisingly, for all L_S [75].

The origin of the unusual behavior of the scattering processes, expressed both in Fig. 2 and Eqs. (2), is directly connected to the special structure of the finite topological Josephson junction under study. First, due to the helical nature of the 2DTI edge states, the junction hosts a pair of topological ABSs for any L_S [50]. Moreover, owing to the finite length, $2L_S$, the system traps discrete levels, which, however, only emerge for $|\omega| > \Delta$ and therefore do not affect transport within the gap. Thus, the Andreev reflected hole (electron) in the leftmost N, characterized by $r_{eh(he)}$, actually carries all the information of a full closed cycle within the finite junction, including transmission across $x = L_S$ and Andreev reflection at $x = 2L_S$. As a consequence, the numerator of $r_{eh(he)}$ acquires a $(1 + e^{-i\phi})$ phase dependence, making it vanish at $\phi = \pi$. Moreover, we have verified that in the absence of the rightmost N region, i.e., when the right S region is instead semi-infinite, the effect of ϕ on r_{eh} becomes a global complex phase, thus leaving no information about the topological ABSs in the Andreev probability $|r_{eh}|^2$. Hence, the interface at $x = 2L_S$, which defines the finite length of the S regions, is absolutely necessary to reveal the formation of topological ABSs at $x = L_S$ in the scattering probabilities and thus also in the conductance.

To summarize, local and nonlocal conductance measurements, set directly by the local Andreev reflection and normal transmission, respectively, are enough to detect the formation of topological ABSs, thus also revealing the presence of MZMs at $\phi = \pi$. Since equilibrium transport in superconducting junctions involves the transfer of Cooper pairs for subgap frequencies, it is natural to next ask about the symmetry of the Cooper pairs that creates these striking transport features.

III. INDUCED ODD-ω PAIRS

We next investigate the symmetries of the induced Cooper pairs in the junction by analyzing the superconducting pair amplitudes. In general, the pair amplitudes are obtained from the electron-hole (eh) part of the retarded Green's function G^r [4,5], which satisfies $[\omega - H_{BdG}(x)]G^r(x, x', \omega) = \delta(x - x')$, where H_{BdG} is a matrix in spin and Nambu spaces given by Eq. (1). To obtain G^r, we follow the method based on scattering states [15,16,21,76–80], which here involves only local Andreev reflections and normal transmissions; for details, see Ref. [67]. To identify the symmetries of the pair amplitude $[G^r(x, x', \omega)]_{eh}$, we inspect its dependence on frequency, spin, and spatial coordinates. The spin symmetry is immediately evident by writing $G^r_{eh} = \sum_i F^r_j \sigma_i$, with $j = 0, \cdots, 3$. Here, F^r_0 is the spin-singlet (S), while $F^r_{1,2,3}$ are the equal- ($j = 1, 2$) and mixed-spin ($j = 3$) triplet (T) states. Moreover, we are interested in finding Cooper pair signatures in transport observables measured locally at the interfaces $x = 0, 2L_S$. We also know from the previous section that transport is governed
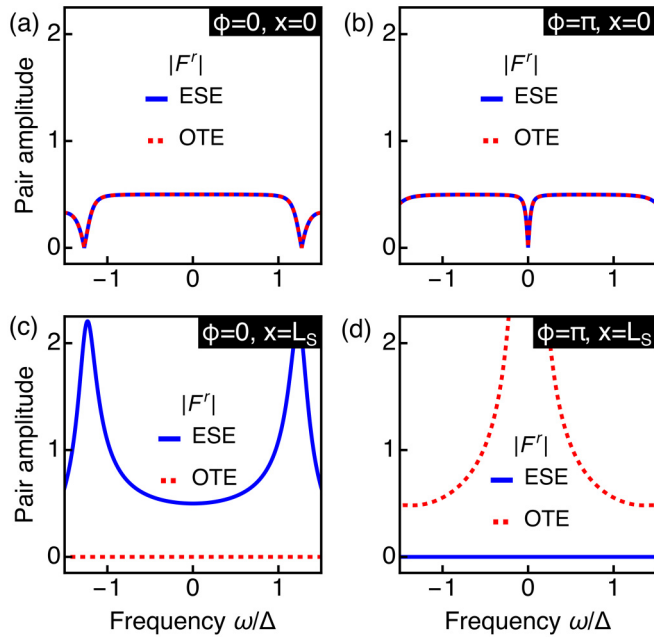
FIG. 3. (a)–(d) Absolute value of the local ESE and OTE pair amplitudes inside the topological Josephson junction as a function of ω at $\phi = 0, \pi$ for $x = 0$ (a), (b) and $x = L_S$ (c), (d). Parameters same as Fig. 2: $\mu = \Delta$, $L_S = 2\xi$.

by the topological ABSs that locally reside at $x = L_S$. It is therefore most interesting to focus on the local pairs at these interfaces, i.e., those that are finite for $x = x'$, which means only considering even-parity (E) spatial symmetry. Hence, taking into account that the Cooper pair amplitudes must be overall antisymmetric due to Fermi-Dirac statistics, we reduce all the possible symmetries to just two local pair symmetries: even-ω spin-singlet even-parity (ESE) and odd-ω spin-triplet even-parity (OTE) [81]. Below we discuss the emergence of these two local pair symmetries in the junction of Fig. 1(a), with details presented in Ref. [67].

Under general conditions, we find finite local pair amplitudes with ESE (OTE) symmetry in all regions of the junction, denoted here as $F^{r,\text{E(O)}}$, respectively. While the ESE symmetry is in the spin-singlet state of the parent superconductor, the OTE symmetry is in the mixed spin-triplet state and emerges due to the strong spin-momentum locking in 2DTI edges [14,21,71,82,83]. The existence of these two pair symmetries in both the N and S regions is determined by the scattering processes at the junction interfaces, which also introduce a strong dependence on the superconducting phase difference ϕ. At the outer interfaces ($x = 0, 2L_S$), ESE and OTE pairs are simultaneously determined by the same local Andreev reflection, making it essentially impossible to distinguish between these two types of Cooper pairs. This effect is seen in Figs. 3(a) and 3(b), which depict the frequency dependence of ESE and OTE amplitudes at $x = 0$ for $\phi = 0$ and π, respectively. While at $\phi = 0$ both ESE and OTE pairs are finite and constant for $|\omega| < \Delta$, at $\phi = \pi$ both amplitudes develop a dip and vanish at $\omega = 0$.

In the middle of the junction, at $x = L_S$, the situation is interestingly distinct to what occurs at the outer interfaces, as seen in Figs. 3(c) and 3(d). At $\phi = 0$ and $x = L_S$, the ESE

term is always finite and also captures the gap edge coherence peaks, while the OTE component completely vanishes. Interestingly, at $\phi = \pi$ and $x = L_S$, the ESE part instead vanishes for all ω, while the OTE term is finite for all ω and even exhibits a resonant profile at $\omega = 0$, thus becoming both large and the only type of superconducting pairing. The resonant OTE profile results from the protected crossing of the topological ABSs at zero frequency and also reflects the dynamical symmetry of this superconducting state. Indeed, we find that the pair amplitudes at $x = L_S$ are fully determined by the scattering processes, which include the ABSs through the zeros of the denominator of the scattering matrix [21,70,71]. We have thus identified that, while under general circumstances Cooper pairs with both ESE and OTE symmetries coexist, only pairs with OTE symmetry remain in the middle of the junction at $\phi = \pi$ and $\omega = 0$ [84].

Having established the emergence and dominant behavior of OTE Cooper pairs at $\phi = \pi$, we finally address their connection to the transport observables discussed in the previous section. Since electron transport at subgap frequencies involves only the transfer of Cooper pairs, the signatures in the Andreev reflection and transmission necessarily correspond to the dominant OTE Cooper pair symmetry. This is also supported by the fact that the origin of the dominant OTE symmetry, the topological ABSs, is the same as that of the dip and resonant profile in the local Andreev and transmission probabilities at zero frequency, see Figs. 2(b) and 2(d), respectively. As a consequence, a clear signature of OTE Cooper pairs is measuring at $\phi = \pi$ either a dip in the local conductance, related to Andreev reflection, or a peak of the nonlocal conductance, determined by normal transmissions. Due to the topological protection of the zero-energy ABS at $\phi = \pi$, our results remain valid also for longer N regions. In fact, for any N region shorter than the superconducting coherence length, no other states appear in the N region which can modify the results [21,72–74]. We have further verified that our results remain overall robust even for longer N regions and also for S regions of distinct lengths [67].

In conclusion, we have identified the impact of Cooper pair symmetries in transport observables in a N-SNS-N topological Josephson junction at the edge of a 2D topological insulator. In particular, we have found vanishing local Andreev reflection and perfect normal transmission at $\phi = \pi$ and $\omega = 0$ as a result of the interplay between the finite junction size and the emergence of a pair of topological ABSs. Furthermore, we have discovered that the Cooper pairs responsible for this surprising transport behavior only have odd-frequency mixed spin-triplet symmetry in the middle of the junction. We note that very similar short Josephson junctions at the edge of 2D topological insulators as proposed here have already been fabricated with good proximity-induced superconductivity in, e.g., HgCd/HgTe and InAs/GaSb [56–59,85]. In these systems, there is also evidence of having achieved phase tuning to $\phi = \pi$ through the measurement of the 4π fractional Josephson effect [57–59]. Moreover, conductance measurements have also been performed in these systems [55,56,58,85]. Taken together, these recent results place our proposal clearly within experimental reach. Our work thus paves the way for highly controllable detection

schemes of odd-frequency pairing in topological Josephson junctions.

[1] A. Acín, I. Bloch, H. Buhrman, T. Calarco, C. Eichler, J. Eisert, D. Esteve, N. Gisin, S. J. Glaser, F. Jelezko, S. Kuhr, M. Lewenstein, M. F. Riedel, P. O. Schmidt, R. Thew, A. Wallraff, I. Walmsley, and F. K. Wilhelm, The quantum technologies roadmap: a european community view, New J. Phys. **20**, 080201 (2018).

[2] Y. Tanaka, M. Sato, and N. Nagaosa, Symmetry and topology in superconductors -odd-frequency pairing and edge states-, J. Phys. Soc. Jpn. **81**, 011013 (2012).

[3] J. Linder and A. V. Balatsky, Odd-frequency superconductivity, Rev. Mod. Phys. **91**, 045005 (2019).

[4] C. Triola, J. Cayao, and A. M. Black-Schaffer, The role of odd-frequency pairing in multiband superconductors, Ann. Phys. **532**, 1900298 (2020).

[5] J. Cayao, C. Triola, and A. M. Black-Schaffer, Odd-frequency superconducting pairing in one-dimensional systems, Eur. Phys. J.: Spec. Top. **229**, 545 (2020).

[6] V. L. Berezinskii, New model of the anisotropic phase of superfluid ^{3}He, Zh. Eksp. Teor. Fiz. **20**, 628 (1974) [JETP Lett. **20**, 287 (1974)].

[7] A. Balatsky and E. Abrahams, New class of singlet superconductors which break the time reversal and parity, Phys. Rev. B **45**, 13125 (1992).

[8] E. Abrahams, A. Balatsky, D. J. Scalapino, and J. R. Schrieffer, Properties of odd-gap superconductors, Phys. Rev. B **52**, 1271 (1995).

[9] F. S. Bergeret, A. F. Volkov, and K. B. Efetov, Long-Range Proximity Effects in Superconductor-Ferromagnet Structures, Phys. Rev. Lett. **86**, 4096 (2001).

[10] Y. Tanaka, Y. Tanuma, and A. A. Golubov, Odd-frequency pairing in normal-metal/superconductor junctions, Phys. Rev. B **76**, 054522 (2007).

[11] A. Kadigrobov, R. I. Shekhter, and M. Jonson, Quantum spin fluctuations as a source of long-range proximity effects in diffusive ferromagnet-superconductor structures, Europhys. Lett. **54**, 394 (2001).

[12] A. M. Black-Schaffer and A. V. Balatsky, Odd-frequency superconducting pairing in topological insulators, Phys. Rev. B **86**, 144506 (2012).

[13] A. M. Black-Schaffer and A. V. Balatsky, Proximity-induced unconventional superconductivity in topological insulators, Phys. Rev. B **87**, 220506(R) (2013).

[14] F. Crépin, P. Burset, and B. Trauzettel, Odd-frequency triplet superconductivity at the helical edge of a topological insulator, Phys. Rev. B **92**, 100507(R) (2015).

[15] B. Lu, P. Burset, K. Yada, and Y. Tanaka, Tunneling spectroscopy and Josephson current of superconductor-ferromagnet hybrids on the surface of a 3D TI, Supercond. Sci. Technol. **28**, 105001 (2015).

[16] P. Burset, B. Lu, G. Tkachov, Y. Tanaka, E. M. Hankiewicz, and B. Trauzettel, Superconducting proximity effect in three-dimensional topological insulators in the presence of a magnetic field, Phys. Rev. B **92**, 205424 (2015).

[17] S. H. Jacobsen, I. Kulagina, and J. Linder, Controlling superconducting spin flow with spin-flip immunity using a single homogeneous ferromagnet, Sci. Rep. **6**, 23926 (2016).

[18] B. Lu, P. Burset, Y. Tanuma, A. A. Golubov, Y. Asano, and Y. Tanaka, Influence of the impurity scattering on charge transport in unconventional superconductor junctions, Phys. Rev. B **94**, 014504 (2016).

[19] O. Kashuba, B. Sothmann, P. Burset, and B. Trauzettel, Majorana STM as a perfect detector of odd-frequency superconductivity, Phys. Rev. B **95**, 174516 (2017).

[20] P. Burset, B. Lu, S. Tamura, and Y. Tanaka, Current fluctuations in unconventional superconductor junctions with impurity scattering, Phys. Rev. B **95**, 224502 (2017).

[21] J. Cayao and A. M. Black-Schaffer, Odd-frequency superconducting pairing and subgap density of states at the edge of a two-dimensional topological insulator without magnetism, Phys. Rev. B **96**, 155426 (2017).

[22] C. Fleckenstein, N. T. Ziani, and B. Trauzettel, Conductance signatures of odd-frequency superconductivity in quantum spin Hall systems using a quantum point contact, Phys. Rev. B **97**, 134523 (2018).

[23] S.-Y. Hwang, P. Burset, and B. Sothmann, Odd-frequency superconductivity revealed by thermopower, Phys. Rev. B **98**, 161408(R) (2018).

[24] D. Kuzmanovski, R. S. Souto, and A. V. Balatsky, Odd-frequency superconductivity near a magnetic impurity in a conventional superconductor, Phys. Rev. B **101**, 094505 (2020).

[25] D. Kuzmanovski, A. M. Black-Schaffer, and J. Cayao, Suppression of odd-frequency pairing by phase disorder in a nanowire coupled to Majorana zero modes, Phys. Rev. B **101**, 094506 (2020).

[26] T. Savander, S. Tamura, C. Flindt, Y. Tanaka, and P. Burset, Thermoelectric detection of Andreev states in unconventional superconductors, Phys. Rev. Research **2**, 043388 (2020).

[27] J. A. Krieger, A. Pertsova, S. R. Giblin, M. Döbeli, T. Prokscha, C. W. Schneider, A. Suter, T. Hesjedal, A. V. Balatsky, and Z. Salman, Proximity-Induced Odd-Frequency Superconductivity in a Topological Insulator, Phys. Rev. Lett. **125**, 026802 (2020).

[28] V. Perrin, F. L. N. Santos, G. C. Ménard, C. Brun, T. Cren, M. Civelli, and P. Simon, Unveiling Odd-Frequency Pairing

Around a Magnetic Impurity in a Superconductor, Phys. Rev. Lett. **125**, 117003 (2020).

[29] S. Pal and C. Benjamin, Exciting odd-frequency equal-spin triplet correlations at metal-superconductor interfaces, Phys. Rev. B **104**, 054519 (2021).

[30] M. Eschrig, T. Löfwander, T. Champel, J. C. Cuevas, J. Kopu, and G. Schön, Symmetries of pairing correlations in superconductor–ferromagnet nanostructures, J. Low Temp. Phys. **147**, 457 (2007).

[31] P. Burset, B. Lu, H. Ebisu, Y. Asano, and Y. Tanaka, All-electrical generation and control of odd-frequency s-wave cooper pairs in double quantum dots, Phys. Rev. B **93**, 201402(R) (2016).

[32] J. Cayao and A. M. Black-Schaffer, Odd-frequency superconducting pairing in junctions with Rashba spin-orbit coupling, Phys. Rev. B **98**, 075425 (2018).

[33] P. Dutta and A. M. Black-Schaffer, Signature of odd-frequency equal-spin triplet pairing in the Josephson current on the surface of Weyl nodal loop semimetals, Phys. Rev. B **100**, 104511 (2019).

[34] R. Seoane Souto, D. Kuzmanovski, and A. V. Balatsky, Signatures of odd-frequency pairing in the Josephson junction current noise, Phys. Rev. Research **2**, 043193 (2020).

[35] F. L. N. Santos, V. Perrin, F. Jamet, M. Civelli, P. Simon, M. C. O. Aguiar, E. Miranda, and M. J. Rozenberg, Odd-frequency superconductivity in dilute magnetic superconductors, Phys. Rev. Research **2**, 033229 (2020).

[36] L. G. Johnsen and J. Linder, Spin injection and spin relaxation in odd-frequency superconductors, Phys. Rev. B **104**, 144513 (2021).

[37] F. Schrodi, A. Aperis, and P. M. Oppeneer, Induced odd-frequency superconducting state in vertex-corrected Eliashberg theory, Phys. Rev. B **104**, 174518 (2021).

[38] V. Kornich, F. Schlawin, M. A. Sentef, and B. Trauzettel, Direct detection of odd-frequency superconductivity via time- and angle-resolved photoelectron fluctuation spectroscopy, Phys. Rev. Research **3**, L042034 (2021).

[39] F. S. Bergeret, A. F. Volkov, and K. B. Efetov, Odd triplet superconductivity and related phenomena in superconductor-ferromagnet structures, Rev. Mod. Phys. **77**, 1321 (2005).

[40] M. Eschrig, Spin-polarized supercurrents for spintronics: A marriage between superconductivity and ferromagnetism is opening the door for new spin-based applications, Phys. Today **64**, 43 (2011).

[41] J. Linder and J. W. A. Robinson, Superconducting spintronics, Nat. Phys. **11**, 307 (2015).

[42] M. Eschrig, Spin-polarized supercurrents for spintronics: a review of current progress, Rep. Prog. Phys. **78**, 104501 (2015).

[43] G. Yang, C. Ciccarelli, and J. W. Robinson, Boosting spintronics with superconductivity, APL Mater. **9**, 050703 (2021).

[44] A. D. Bernardo, S. Diesch, Y. Gu, J. Linder, G. Divitini, C. Ducati, E. Scheer, M. Blamire, and J. Robinson, Signature of magnetic-dependent gapless odd frequency states at superconductor/ferromagnet interfaces, Nat. Commun. **6**, 8053 (2015).

[45] A. Di Bernardo, Z. Salman, X. L. Wang, M. Amado, M. Egilmez, M. G. Flokstra, A. Suter, S. L. Lee, J. H. Zhao, T. Prokscha, E. Morenzoni, M. G. Blamire, J. Linder, and J. W. A. Robinson, Intrinsic Paramagnetic Meissner Effect Due to s-Wave Odd-Frequency Superconductivity, Phys. Rev. X **5**, 041021 (2015).

[46] K. Flensberg, F. von Oppen, and A. Stern, Engineered platforms for topological superconductivity and Majorana zero modes, Nat. Rev. Mater. **6**, 944 (2021).

[47] S. Tamura, S. Hoshino, and Y. Tanaka, Generalization of spectral bulk-boundary correspondence, Phys. Rev. B **104**, 165125 (2021).

[48] S. D. Sarma, M. Freedman, and C. Nayak, Majorana zero modes and topological quantum computation, npj Quantum Inf. **1**, 15001 (2015).

[49] L. Fu and C. L. Kane, Superconducting Proximity Effect and Majorana Fermions at the Surface of a Topological Insulator, Phys. Rev. Lett. **100**, 096407 (2008).

[50] L. Fu and C. L. Kane, Josephson current and noise at a superconductor/quantum-spin-Hall-insulator/superconductor junction, Phys. Rev. B **79**, 161408(R) (2009).

[51] M. Z. Hasan and C. L. Kane, Colloquium: Topological insulators, Rev. Mod. Phys. **82**, 3045 (2010).

[52] X.-L. Qi and S.-C. Zhang, Topological insulators and superconductors, Rev. Mod. Phys. **83**, 1057 (2011).

[53] G. Tkachov and E. M. Hankiewicz, Spin-helical transport in normal and superconducting topological insulators, Phys. Status Solidi B **250**, 215 (2013).

[54] Y. Ando, Topological insulator materials, J. Phys. Soc. Jpn. **82**, 102001 (2013).

[55] I. Knez, R.-R. Du, and G. Sullivan, Andreev Reflection of Helical Edge Modes in InAs/GaSb Qantum Spin Hall Insulator, Phys. Rev. Lett. **109**, 186603 (2012).

[56] S. Hart, H. Ren, T. Wagner, P. Leubner, M. Mühlbauer, C. Brüne, H. Buhmann, L. W. Molenkamp, and A. Yacoby, Induced superconductivity in the quantum spin Hall edge, Nat. Phys. **10**, 638 (2014).

[57] J. Wiedenmann, E. Bocquillon, R. S. Deacon, S. Hartinger, O. Herrmann, T. M. Klapwijk, L. Maier, C. Ames, C. Brüne, C. Gould, A. Oiwa, K. Ishibashi, S. Tarucha, H. Buhmann, and L. W. Molenkamp, 4π-periodic Josephson supercurrent in HgTe-based topological Josephson junctions, Nat. Commun. **7**, 10303 (2016).

[58] E. Bocquillon, R. S. Deacon, J. Wiedenmann, P. Leubner, T. M. Klapwijk, C. Brüne, K. Ishibashi, H. Buhmann, and L. W. Molenkamp, Gapless Andreev bound states in the quantum spin Hall insulator HgTe, Nat. Nanotechnol. **12**, 137 (2017).

[59] R. S. Deacon, J. Wiedenmann, E. Bocquillon, F. Domínguez, T. M. Klapwijk, P. Leubner, C. Brüne, E. M. Hankiewicz, S. Tarucha, K. Ishibashi, H. Buhmann, and L. W. Molenkamp, Josephson Radiation from Gapless Andreev Bound States in HgTe-Based Topological Junctions, Phys. Rev. X **7**, 021011 (2017).

[60] E. Sajadi, T. Palomaki, Z. Fei, W. Zhao, P. Bement, C. Olsen, S. Luescher, X. Xu, J. A. Folk, and D. H. Cobden, Gate-induced superconductivity in a monolayer topological insulator, Science **362**, 922 (2018).

[61] V. Fatemi, S. Wu, Y. Cao, L. Bretheau, Q. D. Gibson, K. Watanabe, T. Taniguchi, R. J. Cava, and P. Jarillo-Herrero, Electrically tunable low-density superconductivity in a monolayer topological insulator, Science **362**, 926 (2018).

[62] C. L. Kane and E. J. Mele, Quantum Spin Hall Effect in Graphene, Phys. Rev. Lett. **95**, 226801 (2005).

[63] J. Alicea, New directions in the pursuit of Majorana fermions in solid state systems, Rep. Prog. Phys. **75**, 076501 (2012).

[64] D. Culcer, A. C. Keser, Y. Li, and G. Tkachov, Transport in two-dimensional topological materials: Recent developments in experiment and theory, 2D Mater. **7**, 022007 (2020).

[65] To obtain perfect 1D metallic edges in 2DTIs, it is beneficial to have large width sample such that the width is much larger than the localization length of the edge states, such as in Ref. [85].

[66] C.-A. Li, J. Li, and S.-Q. Shen, Majorana-Josephson interferometer, Phys. Rev. B **99**, 100504(R) (2019).

[67] See Supplemental Material at http://link.aps.org/supplemental/10.1103/PhysRevB.106.L100502 which includes Ref. [58], for details on the calculation of the scattering and pair amplitudes.

[68] P. Adroguer, C. Grenier, D. Carpentier, J. Cayssol, P. Degiovanni, and E. Orignac, Probing the helical edge states of a topological insulator by cooper-pair injection, Phys. Rev. B **82**, 081303(R) (2010).

[69] G. Tkachov and E. M. Hankiewicz, Helical Andreev bound states and superconducting klein tunneling in topological insulator Josephson junctions, Phys. Rev. B **88**, 075401 (2013).

[70] C. Beenakker, Three "universal" mesoscopic Josephson effects, in *Transport Phenomena in Mesoscopic Systems: Proceedings of the 14th Taniguchi Symposium, Shima, Japan, November 10-14, 1991* (Springer-Verlag, Berlin, Heidelberg, 1992), Vol. 109, p. 235.

[71] F. Keidel, S.-Y. Hwang, B. Trauzettel, B. Sothmann, and P. Burset, On-demand thermoelectric generation of equal-spin cooper pairs, Phys. Rev. Research **2**, 022019(R) (2020).

[72] C. W. J. Beenakker, D. I. Pikulin, T. Hyart, H. Schomerus, and J. P. Dahlhaus, Fermion-Parity Anomaly of the Critical Supercurrent in the Quantum Spin-Hall Effect, Phys. Rev. Lett. **110**, 017003 (2013).

[73] F. Crépin and B. Trauzettel, Parity Measurement in Topological Josephson Junctions, Phys. Rev. Lett. **112**, 077002 (2014).

[74] F. Crépin, B. Trauzettel, and F. Dolcini, Signatures of Majorana bound states in transport properties of hybrid structures based on helical liquids, Phys. Rev. B **89**, 205115 (2014).

[75] For S regions of different lengths, Eqs. (2) acquire more complicated forms but still develop a dip (peak) for Andreev

(transmission) probabilities, albeit their height and width reduce and increase, respectively, see [67] for details.

[76] W. L. McMillan, Theory of superconductor-normal metal interfaces, Phys. Rev. **175**, 559 (1968).

[77] A. Furusaki and M. Tsukada, Dc Josephson effect and Andreev reflection, Solid State Commun. **78**, 299 (1991).

[78] S. Kashiwaya and Y. Tanaka, Tunnelling effects on surface bound states in unconventional superconductors, Rep. Prog. Phys. **63**, 1641 (2000).

[79] W. J. Herrera, P. Burset, and A. Levy Yeyati, A Green function approach to graphene–superconductor junctions with well-defined edges, J. Phys.: Condens. Matter **22**, 275304 (2010).

[80] B. Lu and Y. Tanaka, Study on Green's function on topological insulator surface, Phil. Trans. R. Soc. A. **376**, 20150246 (2018).

[81] We note that nonlocal pair amplitudes can emerge if we allow for $x \neq x'$. It is then possible to obtain even-ω spin-triplet odd-parity and odd-ω spin-singlet odd-parity pair amplitudes, which are odd under the spatial coordinates [16,21]. These components, however, are only finite inside the S regions and thus do not directly contribute to transport.

[82] F. Keidel, P. Burset, and B. Trauzettel, Tunable hybridization of Majorana bound states at the quantum spin Hall edge, Phys. Rev. B **97**, 075408 (2018).

[83] B. Lu, G. Cheng, P. Burset, and Y. Tanaka, Identifying Majorana bound states at quantum spin Hall edges using a metallic probe, arXiv:2110.04472.

[84] In the case of a topological Josephson junction with a long middle N region, we have verified that the OTE pairing remains the only type of pairing in the middle of such N region, also in agreement with previous findings [21]. For S regions of distinct lengths, a vanishing small ESE component appears but the OTE pairing remains the largest pair amplitude, thus reflecting the dominant character of OTE Cooper pairs, see Ref. [67].

[85] V. S. Pribiag, A. J. A. Beukman, F. Qu, M. C. Cassidy, C. Charpentier, W. Wegscheider, and L. P. Kouwenhoven, Edge-mode superconductivity in a two-dimensional topological insulator, Nat. Nanotechnol. **10**, 593 (2015).